Indian Journal of Pure & Applied Physics
Vol. 64, June 2026, pp. 633-649
DOI: 10.56042/ijpap.v64i6.27506

Iterative Chi-Square Minimization for Gamma Ray Spectrometry: Quantifying K, U and Th concentrations in Geological Samples

Ankur Trivedi[a,b*], H B Shrivastava[a], Uday Kumar[b], G K Sharma[a], R K Mondal[a], N K Johri[a] & S K Dash[a]

[a]Atomic Minerals Directorate for Exploration and Research, Department of Atomic Energy, Jamshedpur 831 002, India

[b]Department of Physics, National Institute of Technology, Jamshedpur 831 014, India

Received: 12th January 2026; accepted: 8th April 2026

Gamma ray spectrometry is widely employed for quantifying naturally occurring radioactive elements such as potassium (K), uranium (U) and thorium (Th) in geological materials. However, conventional energy window based analysis (EWBA) is constrained by spectral overlap and simplified treatment of counting uncertainties. In this study, an iterative chi-square minimization (ICSM) algorithm with adaptive uncertainty refinement is implemented in Python to perform full spectrum analysis of NaI(Tl) gamma ray spectra over the energy range 0.4 – 2.9 MeV. Standard spectrum from International Atomic Energy Agency (IAEA) Standard Reference Materials (SRMs) and a calibrated 5″ x 4″ NaI(Tl) detector are used to determine isotopic concentrations and their uncertainties in a sample spectrum. Elemental response functions derived from reference standards are used to model measured spectra as linear combinations of K, U, and Th contributions, while channel wise uncertainties are iteratively updated based on the expected (fitted) spectrum.

The method is applied to geological samples and to three in-house certified reference materials (CRMs) analyzed as unknowns. For the samples, ICSM consistently yields lower uncertainties than EWBA for identical counting times, with typical uncertainty reductions of approximately 1.3 – 1.8 x for K, 2 – 3 x for U, and 1.5 – 2.5 x for Th. The in-house standards, having concentrations independently determined using a high purity germanium (HPGe) detector, provide an external validation of quantitative performance. ICSM derived concentrations exhibit closer agreement with HPGe reference values and substantially reduced uncertainties compared with EWBA. Residual analysis and reduced chi-square values indicate statistically consistent fits across all analyzed spectra. These results demonstrate that iterative chi-square minimization with adaptive uncertainty refinement offers a precise and statistically robust alternative to window based methods for quantitative gamma ray spectrometric analysis of geological materials.

Keywords: Gamma ray spectrometry, ICSM, NaI(Tl), HPGe

1 Introduction

Naturally occurring radioactive materials (NORM) like K, U and Th are ubiquitous in the Earth's crust and provide valuable insights into geological processes, environmental monitoring and radiation safety. Gamma ray spectrometry[1] is widely used to measure these isotopes due to their distinct gamma ray emission energies. However, these measurements are complicated by spectral overlap and background radiation[2], hence necessitating advanced deconvolution techniques[3]. Traditional methods, such as energy window-based analysis (EWBA)/region of interest (ROI) sometimes struggle to account for overlapping peaks or varying detector efficiencies. Least squares fitting offers a robust alternative by modeling the entire spectrum as a linear combination of standard responses[4]. This study employs an iterative chi-square minimization (ICSM) approach, that refines uncertainty estimates during fitting to improve accuracy. The procedure is applied to sample spectrums obtained in a gamma spectrometry system calibrated against IAEA standards (RGK, RGU, RGTh) to determine isotopic concentrations and assess fit quality.

2 Methodology

2.1 Energy Calibration

Energy calibration[5] is performed using known gamma ray peaks of 0.662 MeV (CS-137), 1.460 MeV (K-40), 1.760 MeV (U-238) and 2.615 MeV (Th-232). The calibration equation obtained from a polynomial fit along with the fitting equation is shown in the calibration curve in Fig. 1. This equation enables conversion of channel numbers to energy values across 1024 channels. Based on this calibration curve, channel filtering is applied for selecting energy range of interest, i.e., 0.4 MeV to 2.9 MeV.

*Corresponding author: E-mail: ankurtrivedi.amd@gov.in

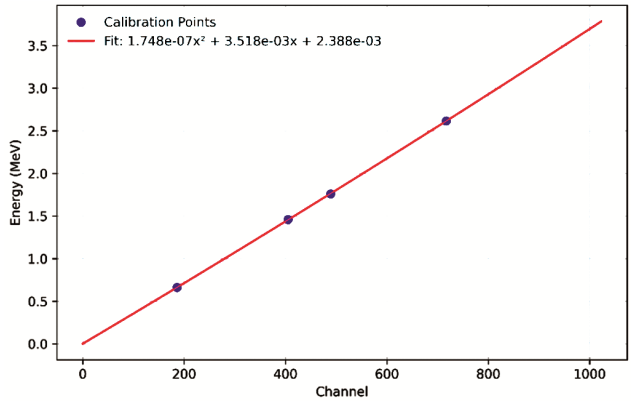

Fig. 1 — Energy calibration curve

2.2 Data Acquisition

Spectral data were collected using a 5″ x 4″ NaI(Tl) detector coupled with a 1024-channel DSP based system. The data set generated includes:

Background Spectrum: Acquired over 36000 seconds to characterize ambient radiation background.

Standard Spectrum: IAEA standards RGK (K_2SO_4, Conc. K = 44.8 %), RGU (Conc. U_3O_8 = 470 ppm) and RGTh (Conc. ThO_2 = 910 ppm) are used to obtain standard spectra with an acquisition time of 1200 seconds for each.

Sample Spectrum: Sample spectrum is acquired for 1200 seconds for seven number of geological samples which have uranium series in secular equilibrium with its daughters and three in-house CRMs analyzed as unknown samples. Acquisition time of 1200 seconds is chosen so that the results can be compared with results of the energy window based (EWB)/ROI analysis of the spectrum for same counting time.

Spectra are acquired over the energy range 0.0 Mev to 3.0 MeV. However, in the study spectrum in the energy range 0.4 MeV to 2.9 MeV are considered as there is a tradeoff between the fitting parameter (goodness of fit) and uncertainty. Increasing the energy range increases the precision but at the cost of fitting errors. Lower spectral width ensures better fit but poor precision. Therefore, an optimum energy range of 0.4 MeV to 2.9 MeV is considered for improved precision and acceptable fit. Moreover, the spectrum in this energy range remains linear, which can be evident from calibration curve. Due to linearity in the selected energy range, energies of 1.46 MeV, 1.76 MeV and 2.62 MeV are conveniently chosen in EWBA method.

2.3 Spectral Processing

All measured spectra are normalized by their respective acquisition times to obtain count rates (counts s^{-1}). The net sample spectrum is computed by subtracting the normalized background spectrum from the normalized sample spectrum:

$$N_i = S_i - BG_i \quad \ldots (1)$$

where N_i, S_i and BG_i denote the net sample, sample and background count rates respectively, in channel i. The response matrix A is constructed from standard spectra measured under identical detector conditions and scaled by their certified concentrations:

$$A = [a_K \;\; a_U \;\; a_{Th}] \quad \ldots (2)$$

where,

$$a_K = \frac{RGK}{C_K}, \quad a_U = \frac{RGU}{C_{U_3O_8}}, \quad a_{Th} = \frac{RGTh}{C_{ThO_2}} \quad \ldots (3)$$

Here, RGK, RGU, and RGTh are the background-corrected standard spectra expressed in counts s^{-1}, and C_K, $C_{U_3O_8}$ and C_{ThO_2} are the corresponding certified concentrations. The response matrix A has dimensions m×3, where m is the number of MCA channels between indices *g* and *h*, corresponding to the energy interval 0.4 – 2.9 MeV determined from the energy calibration curve.

2.4 Iterative Chi-Square Minimization with Adaptive Uncertainty Modeling

An iterative chi-square minimization algorithm is employed to fit the net sample spectrum N as a linear combination of elemental response functions[6]. The objective function minimized is defined as:

$$\chi^2 = \sum_{i=g}^{h} \left(\frac{N_i - (AC)_i}{\sigma_i} \right)^2 \quad \ldots (4)$$

where N_i is the net sample count rate in channel i, $(AC)_i$ is the fitted spectrum, $C = [C_K \; C_U \; C_{Th}]^T$ is the vector of elemental concentrations to be estimated and σ_i is the total uncertainty associated with channel i.

The channel indices *g* and *h* correspond to the lower and upper bounds of the selected energy window and are determined using the energy calibration curve.

2.5 Initial Uncertainty Estimation

An initial estimate of the channel uncertainties is obtained using counting statistics from both the sample and background measurements. Assuming Poisson statistics for the recorded counts, the statistical variance for each channel is given by:

$$\sigma_{i,stat}^2 = \frac{S_i + BG_i}{T_{sample}} + \frac{BG_i}{T_{bg}} \quad \ldots (5)$$

where S_i and BG_i are the sample and background count rates (counts s^{-1}), T_{sample} and T_{bg} are the respective acquisition times. This formulation accounts for counting noise from both the sample and background spectra normalized to count rate.

2.6 Weighted Least-Squares Solution

The fitting problem is solved using a weighted least-squares approach[7], in which channels with lower uncertainty contribute more strongly to the solution. The weights are defined as:

$$w_i=\frac{1}{\sigma_i^2} \quad \ldots (6)$$

These weights form a diagonal weight matrix:

$$W=\text{diag}(w_1,w_2,\ldots,w_m) \quad \ldots (7)$$

While spectral channels are treated as statistically independent for computational tractability, correlations that arise from detector energy resolution are implicitly accommodated through the uncertainty model. The concentration vector is obtained by solving the weighted normal equations:

$$C=(A^TWA)^{-1}A^TWN \quad \ldots (8)$$

To ensure physical consistency, all concentration estimates are constrained to be non-negative:

$$\text{i.e., } C_j \geq 0 \quad \forall\, j \in \{K,U,Th\} \quad \ldots (9)$$

2.7 Iterative Uncertainty Update

The fitted spectrum at iteration t is computed as:

$$M_i^{(t)}=(AC^{(t)}) \quad \ldots (10)$$

Because the true uncertainties depend on the expected rather than observed counts, the uncertainty model is updated using the fitted spectrum. The total variance for each channel can be expressed as the sum of statistical and systematic components[8]:

$$\sigma_i^{2\,(t+1)}=\underbrace{\frac{M_i^{(t)}+BG_i}{T_{sample}}+\frac{BG_i}{T_{bg}}}_{\text{statistical}}+\underbrace{(f\,M_i^{(t)})^2}_{\text{systematic}} \quad \ldots (11)$$

The parameter f represents a fractional systematic uncertainty that accounts for residual detector response mismatch, peak shape variation and calibration imperfections not captured by Poisson counting statistics. A value of $f = 0.05$ is adopted to provide conservative uncertainty estimates and to prevent underestimation of parameter errors. The value of f does not bias the fitted concentrations but inflates the variance to reflect known model imperfections, ensuring that the reduced chi-square remains near unity and that uncertainties are not underestimated.

The updated uncertainties are used to recompute the weights for the next iteration:

$$W^{(t+1)}=\text{diag}\left(\frac{1}{\sigma_1^2},\ldots,\frac{1}{\sigma_m^2}\right)^{(t+1)} \quad \ldots (12)$$

2.8 Convergence Criterion

After each iteration, the chi-square value is recomputed:

$$\chi^2_{(t)}=\sum_{i=g}^{h}\left(\frac{N_i-M_i^{(t)}}{\sigma_i}\right)^2 \quad \ldots (13)$$

Convergence is achieved when the change in chi-square between successive iterations satisfies:

$$\left|\chi^2_{(t+1)}-\chi^2_{(t)}\right| < \varepsilon\ ;\ \varepsilon = 10^{-6} \quad \ldots (14)$$

or when a predefined maximum number of iterations (e.g., 100) is reached.

2.9 Parameter Uncertainties

After convergence of the iterative chi-square minimization procedure, uncertainties associated with the estimated elemental concentrations are derived from the covariance matrix of the weighted least-squares solution:

$$Cov=(A^TWA)^{-1} \quad \ldots (15)$$

where A is the response matrix and W is the diagonal weight matrix constructed from the inverse squared channel uncertainties at convergence. The standard uncertainties (standard errors) of the estimated concentrations are obtained from the square roots of the diagonal elements of the covariance matrix:

$$\Delta C_j=\sqrt{(Cov)_{jj}}\ ;\quad j \in \{K,U,Th\} \quad \ldots (16)$$

These uncertainties reflect the combined influence of statistical counting variability and systematic modeling effects through the adopted uncertainty model.

2.10 Implementation Details

The iterative chi-square minimization algorithm is implemented in Python using matrix operations, statistical analysis and residual diagnostics. A maximum of 100 iterations is imposed to ensure computational efficiency, while a convergence tolerance of 10^{-6} on the change in chi-square balances numerical stability with fitting precision.

Unlike static weighted least squares methods that rely on fixed uncertainty estimates, the present implementation updates channel uncertainties iteratively based on the evolving fitted spectrum. This adaptive uncertainty treatment provides a more realistic representation of expected counting variance, particularly in spectral regions with low count rates or strong background contributions. As a result, the procedure reduces bias associated with uncertainty underestimation and yields more stable parameter estimates and goodness of fit metrics for practical gamma ray spectrometric data.

3 Results

After convergence of the iterative chi-square minimization procedure, elemental concentrations of potassium (K), uranium (U) and thorium (Th) are obtained from the fitted model spectrum. Along with the estimated concentrations, associated uncertainties are derived from the covariance matrix of the weighted least-squares solution. These uncertainties represent the precision of the concentration estimates and reflect the combined effects of counting statistics and systematic modeling contributions incorporated through the adaptive uncertainty model.

The overall quality of the fit is evaluated using the reduced chi-square statistic[9]:

$$\chi_\nu^2=\frac{\chi^2}{\nu} \quad \ldots (17)$$

where the number of degrees of freedom is given by:

$$\nu=N_{ch}-N_{par} \quad \ldots (18)$$

with N_{ch} denoting the number of fitted spectral channels and N_{par} = 3 corresponding to the fitted parameters (K, U, and Th concentrations).

In practical gamma ray spectrometry, detector response functions are approximate and spectral channels are correlated due to finite energy resolution. Consequently, reduced chi-square values moderately greater than unity are expected even for statistically consistent fits. In this work, reduced chi-square values are therefore interpreted in conjunction with residual diagnostics rather than as a strict criterion for model validity.

Residual analysis is performed to identify potential systematic deviations in the fitting process. The normalized residuals,

$$r_i=\frac{N_i-M_i}{\sigma_i} \quad \ldots (19)$$

are examined as a function of energy and through their statistical distribution. For an adequate model, the residuals exhibit no systematic structure and are approximately normally distributed with zero mean. Normal probability (Q–Q) plots are used to assess conformity with the Gaussian assumption underlying the chi-square formulation, providing additional validation of the statistical consistency of the fitted results.

3.1 Concentrations and Uncertainties

Results obtained from the iterative chi-square minimization (ICSM) are tabulated in Table 1 for

Table 1 — Results obtained using iterative χ^2 minimization (ICSM) and Energy window-based analysis (EWBA)

Sample	Method	K (%) ± Err	U (ppm) ± Err	Th (ppm) ± Err
S1	EWBA	0.10 ± 0.18	100 ± 2.43	387 ± 7.47
	ICSM	0.10 ± 0.08	94 ± 1.39	372 ± 3.31
S2	EWBA	1.30 ± 0.62	595 ± 6.00	26 ± 5.80
	ICSM	1.50 ± 0.34	574 ± 2.50	23 ± 2.89
S3	EWBA	2.10 ± 0.30	213 ± 2.88	14 ± 3.11
	ICSM	2.00 ± 0.20	203 ± 1.37	17 ± 2.00
S4	EWBA	2.20 ± 0.39	320 ± 3.79	9 ± 3.43
	ICSM	1.90 ± 0.24	314 ± 1.68	7 ± 2.14
S5	EWBA	1.95 ± 0.45	386 ± 4.32	7 ± 3.85
	ICSM	1.60 ± 0.27	374 ± 1.88	5 ± 2.31
S6	EWBA	0.62 ± 0.21	33 ± 1.80	336 ± 6.79
	ICSM	0.40 ± 0.14	36 ± 1.03	324 ± 2.72
S7	EWBA	5.04 ± 0.20	64 ± 1.60	87 ± 3.54
	ICSM	4.40 ± 0.15	56 ± 0.84	84 ± 1.91
S8	EWBA	4.46 ± 2.89	3576 ± 27.62	86 ± 25.97
	ICSM	0.40 ± 1.48	3624 ± 10.42	15 ± 6.07
S9	EWBA	1.08 ± 1.49	145 ± 11.32	4743 ± 51.14
	ICSM	1.00 ± 0.56	136 ± 4.99	4619 ± 19.92
S10	EWBA	0.22 ± 0.92	1026 ± 8.97	4 ± 0.21
	ICSM	0.15 ± 0.51	1036 ± 3.76	2 ± 0.15

(Error value for K is in %, U in ppm and Th in ppm)

seven number of geological rock samples and three number of in-house certified reference materials (CRMs).

The minimum detectable activity (MDA) of the NaI(Tl) detector for the present measurement geometry are approximately 0.5 % for K, 5 ppm for U and 10 ppm for Th. Concentration values reported below these limits are included solely for methodological comparison between EWBA and ICSM and should not be interpreted as physically meaningful quantitative estimates.

3.2 Spectral Fit

Figures 2 to 11 present the net sample spectra and corresponding fitted spectra for the samples and three in-house CRMs, with channel wise uncertainties shown as error bars. Across the analyzed energy range of 0.4 – 2.9 MeV, the fitted spectra closely reproduce the measured data, capturing both photopeak and continuum features. The agreement between measured and modeled spectra demonstrates the effectiveness of the full spectrum approach in representing overlapping contributions from K, U and Th.

Normalized residuals fluctuate around zero over the entire energy range, with no pronounced systematic structure. Histograms of the normalized residuals are approximately Gaussian, indicating that the uncertainty model provides a reasonable description of the observed variance. Normal probability (Q – Q) plots show residuals lying close to the 1:1 reference line, with minor deviations at the distribution tails. These deviations can be attributed primarily to low count spectral regions and minor unmodeled features, which are common in gamma ray spectrometry.

Although isolated outliers are observed in some samples, the overall residual behavior supports the statistical consistency of the fits and the reliability of the estimated uncertainties. Reduced chi-square values for most samples fall within the range expected for real detector data, where detector response imperfections and channel correlations prevent ideal values of unity. Sample S8 exhibits the highest reduced chi-square value likely due to its higher activity level and increased sensitivity to response mismatches; however,

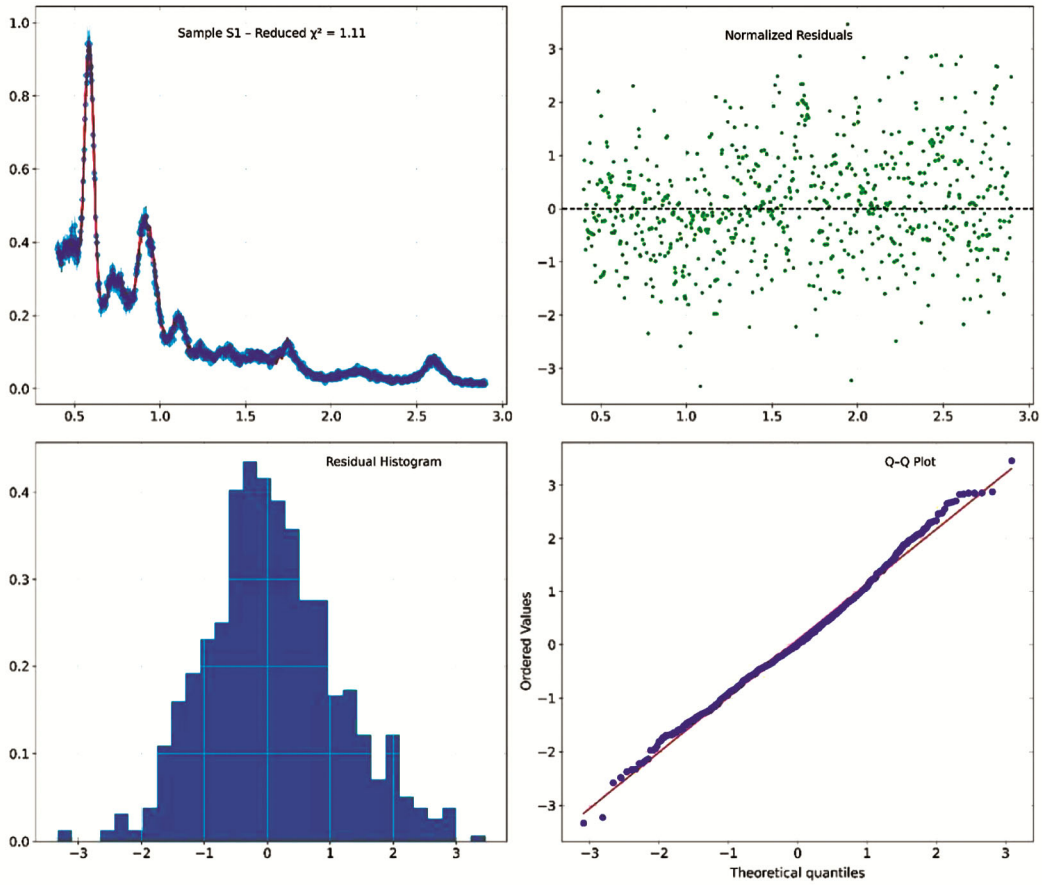

Fig. 2 — Spectral fitting plots for sample S1

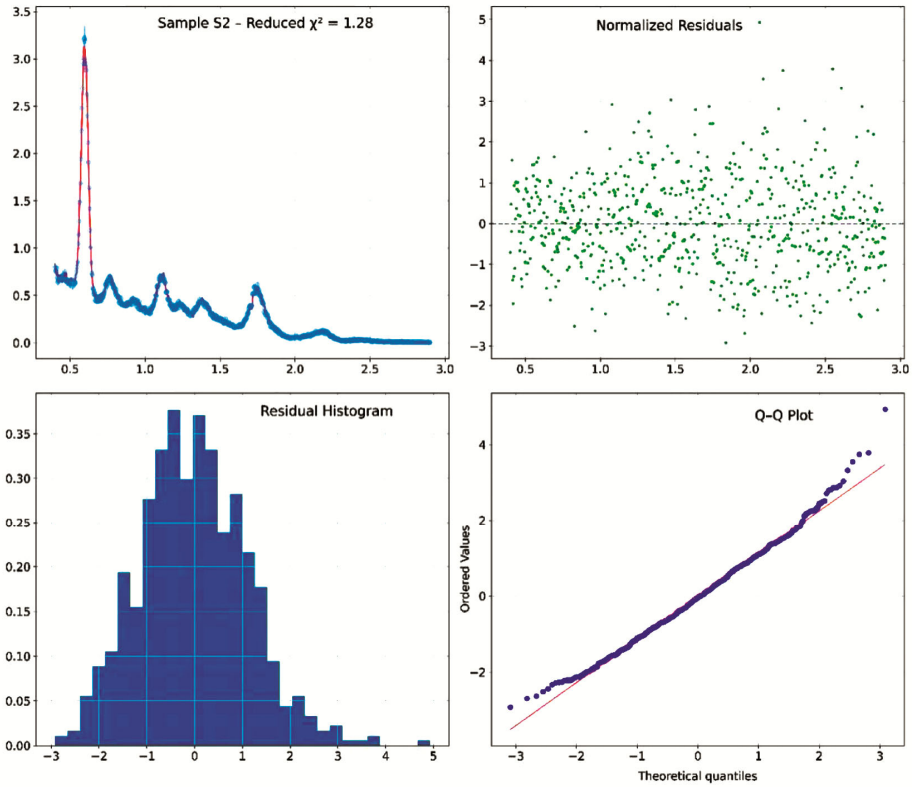

Fig. 3 — Spectral fitting plots for sample S2

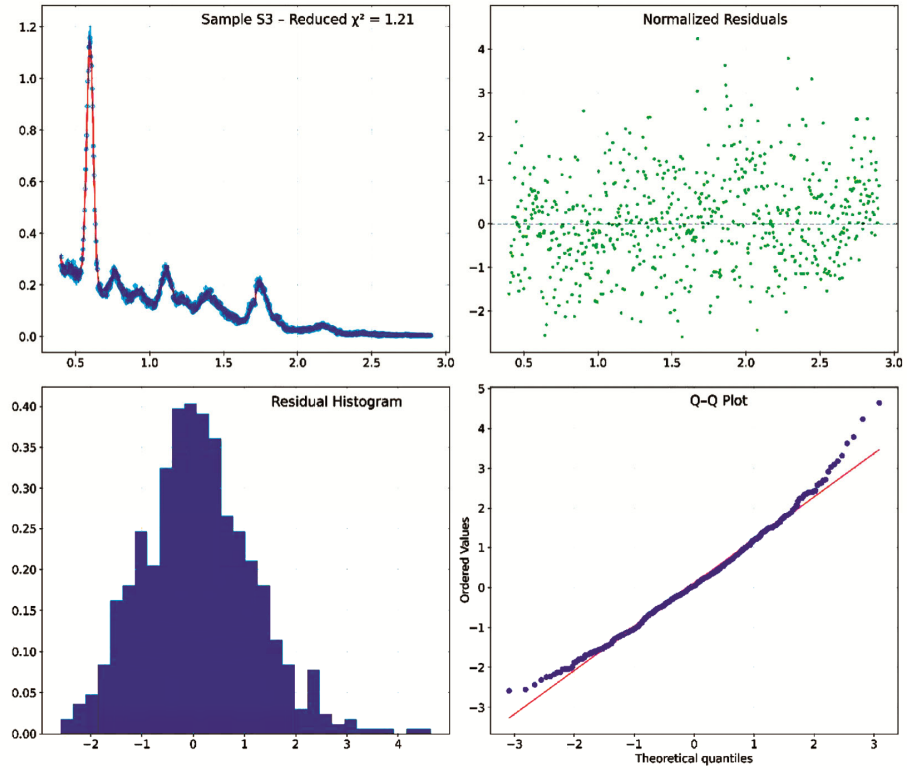

Fig. 4 — Spectral fitting plots for sample S3

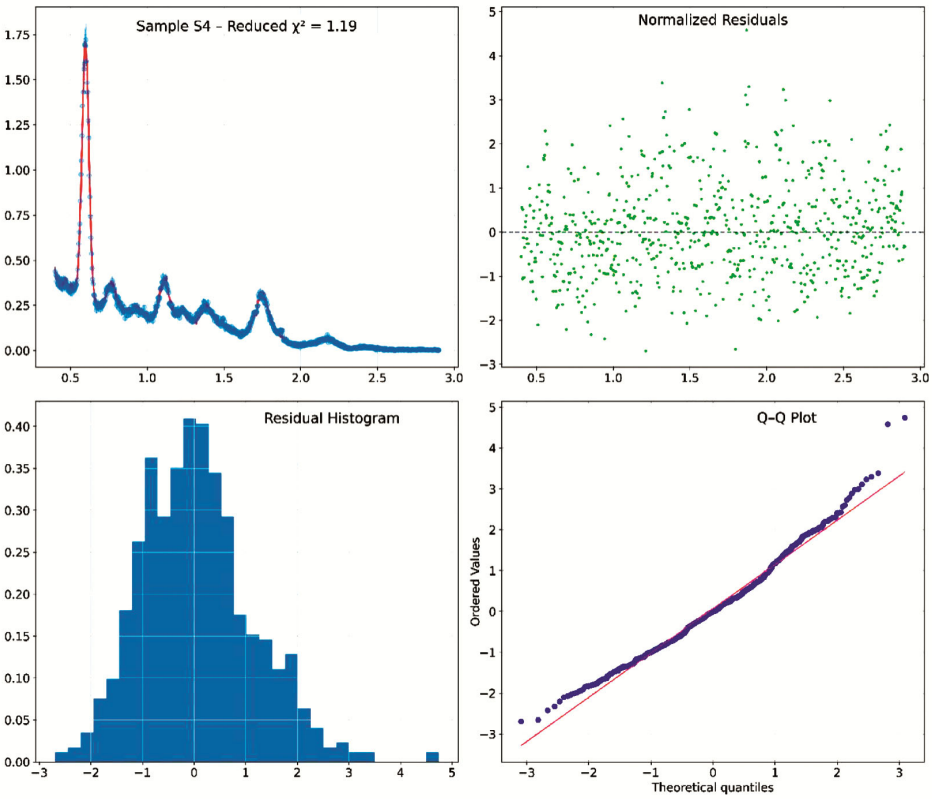

Fig. 5 — Spectral fitting plots for sample S4

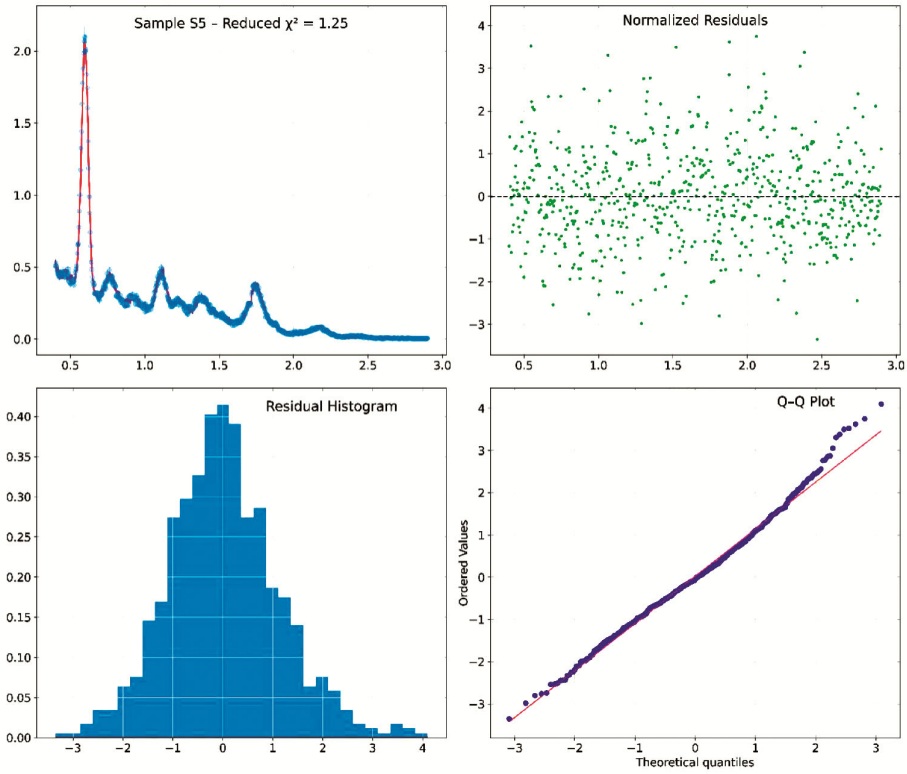

Fig. 6 — Spectral fitting plots for sample S5

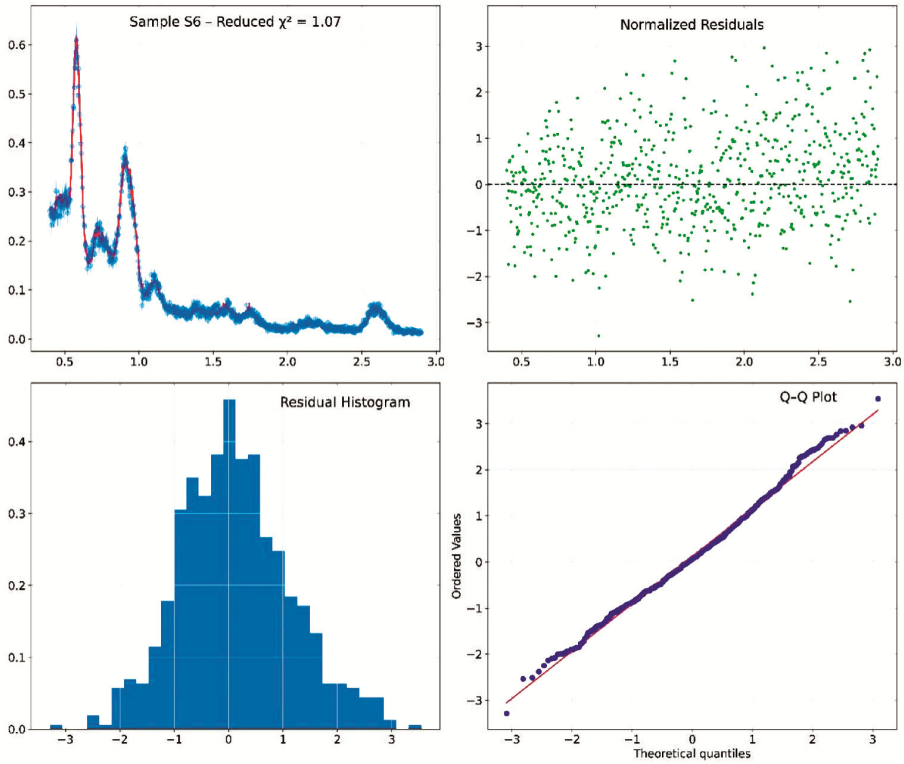

Fig. 7 — Spectral fitting plots for sample S6

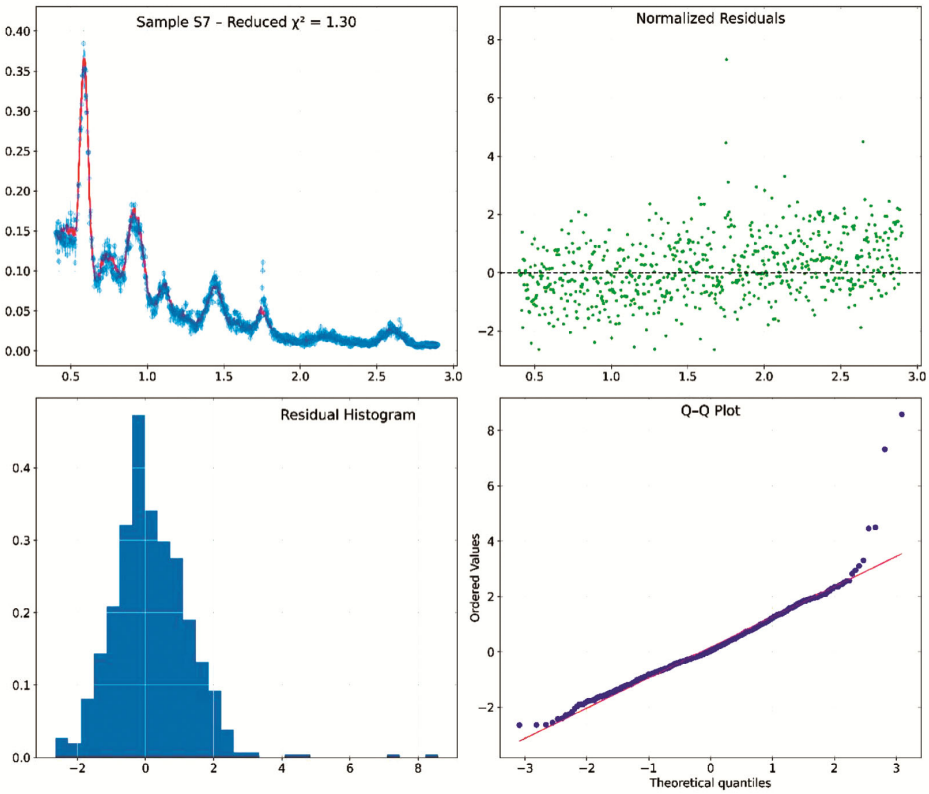

Fig. 8 — Spectral fitting plots for sample S7

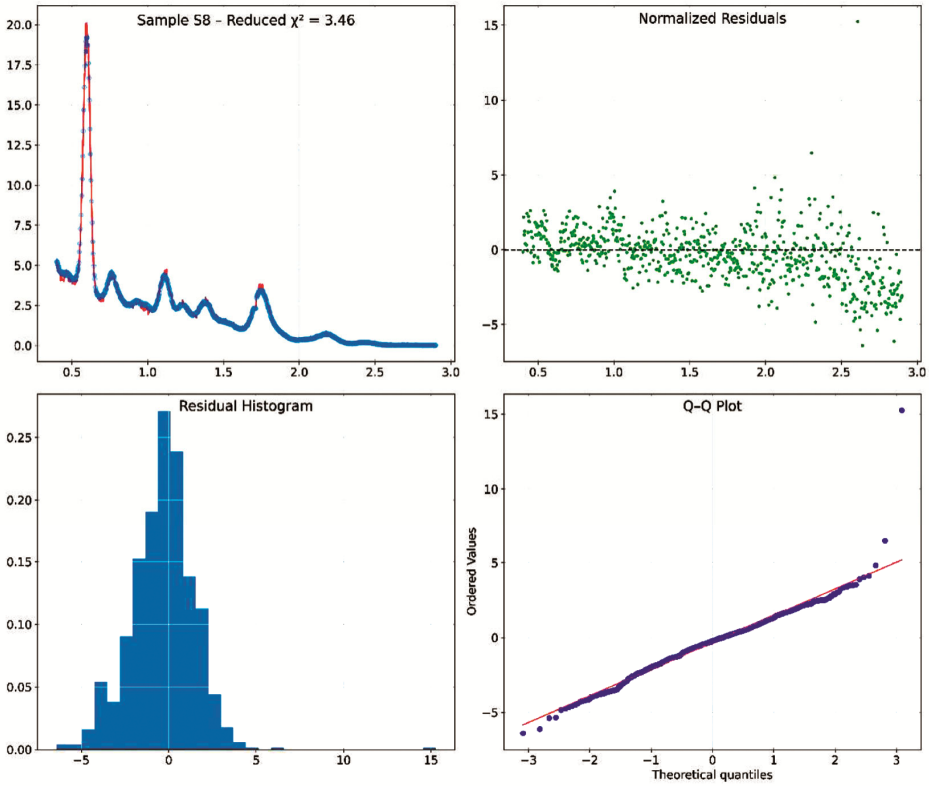

Fig. 9 — Spectral fitting plots for sample S8

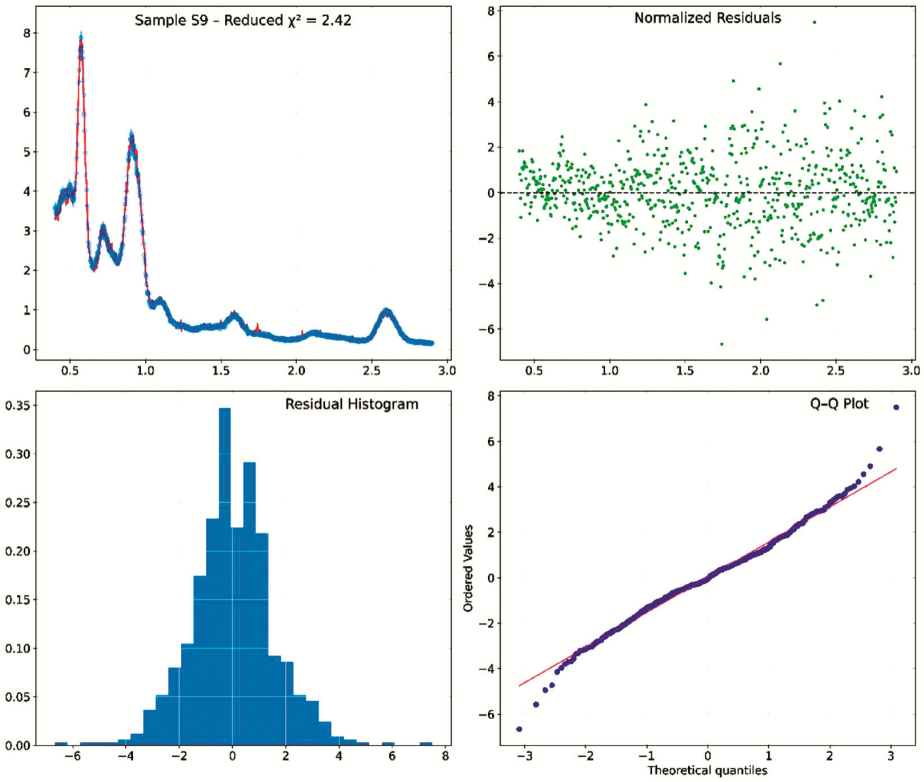

Fig. 10 — Spectral fitting plots for sample S9

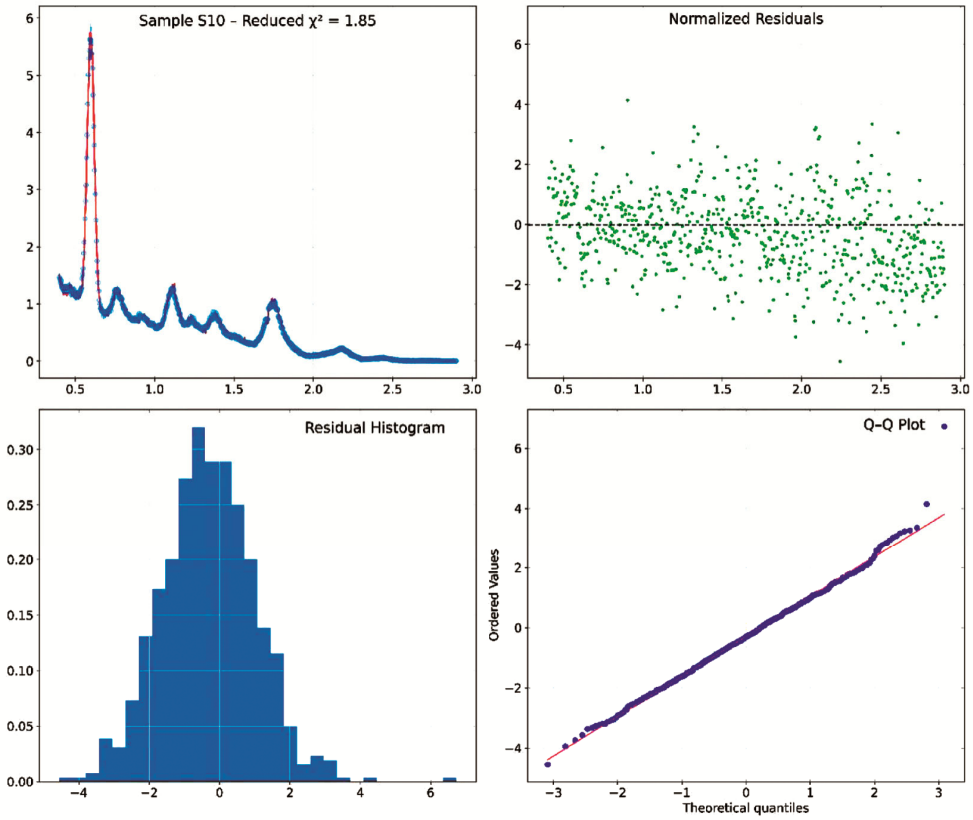

Fig. 11 — Spectral fitting plots for sample S10

the concentrations obtained using the iterative chi-square minimization method remain consistent with those derived from the Energy Window/ROI approach, indicating the robustness of the proposed method even under less ideal fitting conditions.

The choice of energy range from 0.4 MeV to 2.9 MeV is important to make a direct comparison of precision obtained in the two methods. However, to visualize the tradeoff between the fitting parameter (goodness of fit) and energy range a comparative plot is shown for the energy range 0.1 MeV – 2.9 MeV for sample S8 in Fig. 12.

3.3 Comparison with Energy Window Based Analysis (EWBA)/ROI Results

EWBA/ROI result presented earlier and Figs. 13-17 present a comparative analysis. When compared to EWBA/ROI based method, the results obtained in ICSM approach align well which can be inferred from data in Table 2.

The iterative chi-square minimization (ICSM) method demonstrates superior precision compared to the conventional Energy Window Based Analysis (EWBA) by utilizing the entire 0.4–2.9 MeV energy range and fitting the measured spectrum as a linear combination of K, U and Th response functions. By utilizing the full spectral shape, the ICSM approach accounts for spectral overlaps, continuum contributions and background effects, thereby reducing bias and improving the stability of the estimated concentrations. In contrast to static uncertainty models, the iterative uncertainty refinement employed in ICSM updates channel wise uncertainties based on the evolving fitted spectrum, giving a more realistic representation of noise characteristics and improved precision in complex or low-count spectral regions.

The weighted least-squares formulation further enhances precision by assigning greater influence to channels with smaller statistical uncertainty, which are typically associated with higher count rates. EWBA on the other hand integrates counts within narrow regions of interest centered on characteristic photo peaks (e.g., 1.46 MeV for K, 1.76 MeV for U and 2.615 MeV for Th) neglecting spectral overlap and relying on simplified background estimates. Additionally, EWBA commonly employs error propagation based on the square root of integrated

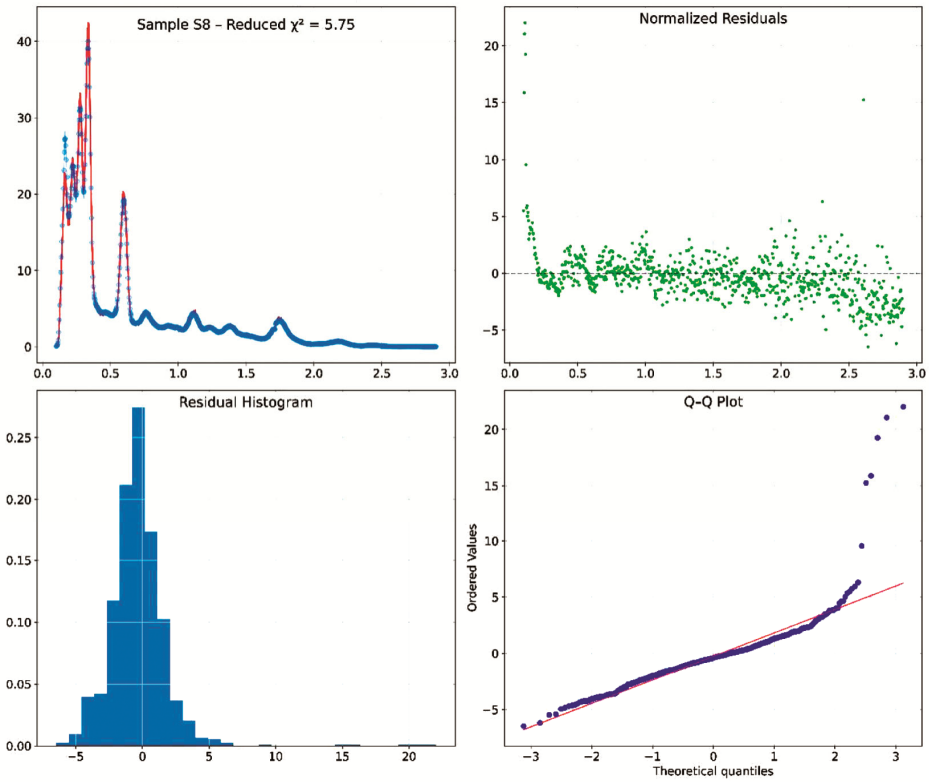

Fig. 12 — Spectral fitting plots for sample S8 (0.1 Mev to Mev)

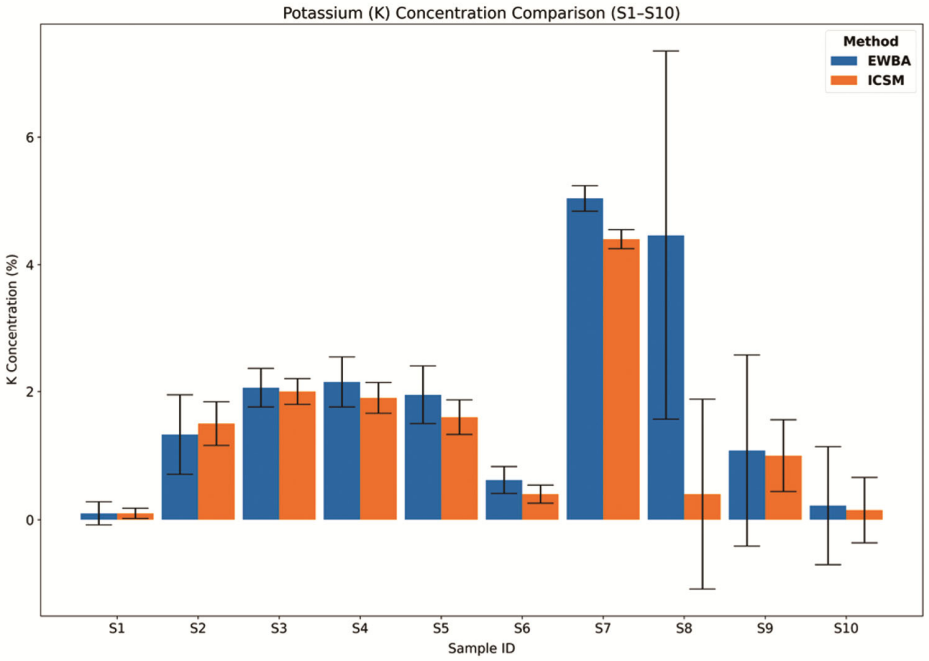

Fig. 13 — K (%) estimation based on EWBA and ICSM methods

counts, which does not adequately capture the effects of spectral interference or correlated uncertainties. As a result, EWBA generally yields larger uncertainties than ICSM. The improved precision achieved using the ICSM method is summarized in Table 3, while Fig. 18 presents a bar chart illustrating the percentage

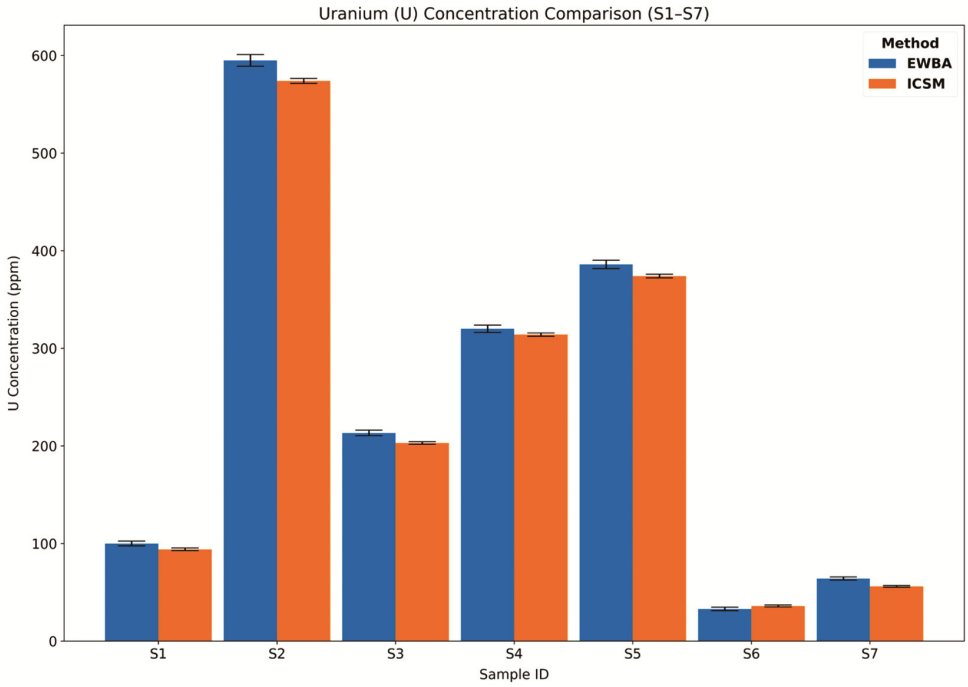

Fig. 14 — U (ppm) estimation based on EWBA and ICSM methods (S1 to S7)

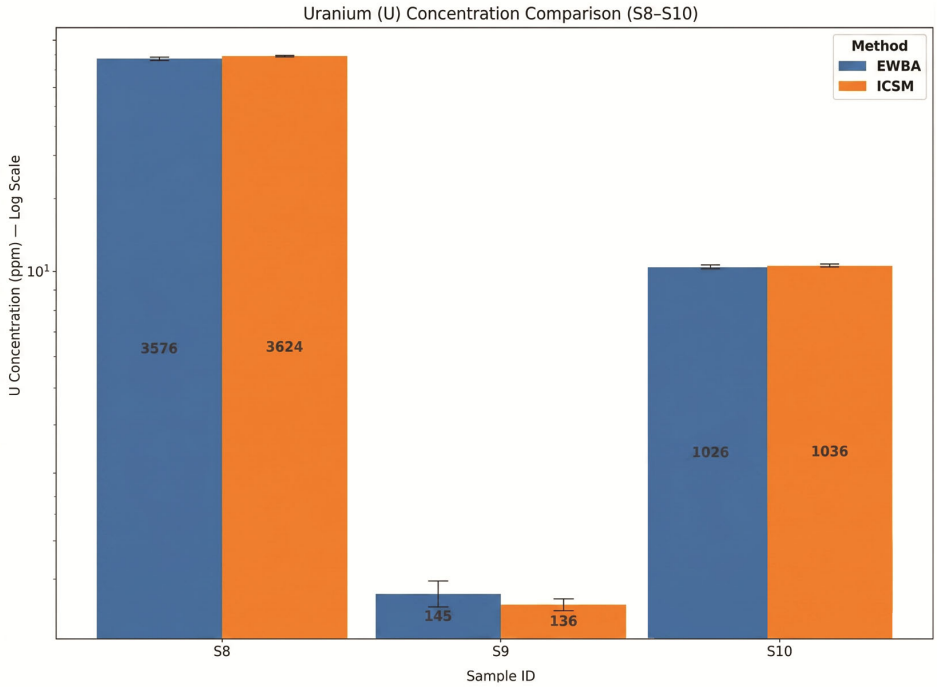

Fig. 15 — U (ppm) estimation based on EWBA and ICSM methods (S8 to S10) Log scale for normalizing the concentrations (actual values mentioned inside bars in ppm)

reduction in uncertainty for K, U and Th across all analyzed samples.

Across the sample set, the reduction in uncertainty achieved by ICSM is substantial, with typical decreases of approximately 30 – 55 % for K, 40 – 65 % for U, and 28 – 55 % for Th relative to EWBA. The improvement in precision is most pronounced for uranium and thorium, reflecting the effectiveness of

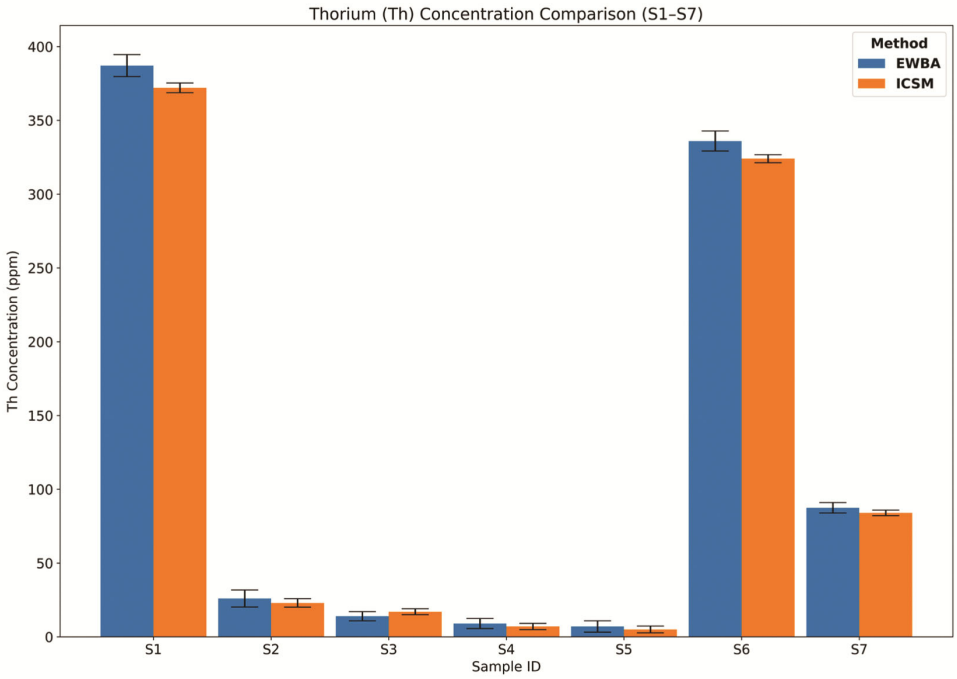

Fig. 16 — Th (ppm) estimation based on EWBA and ICSM methods (S1 to S7)

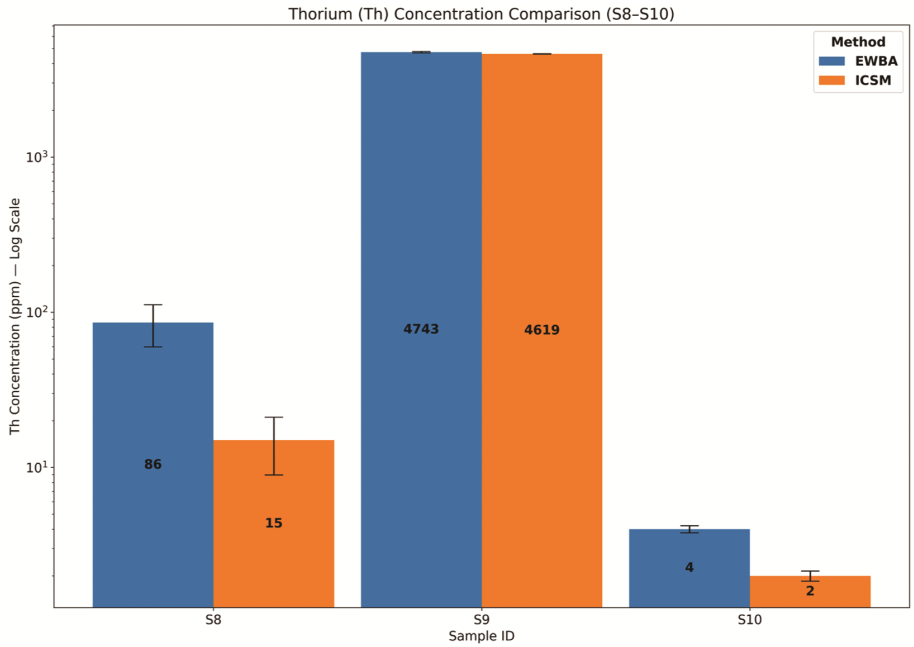

Fig. 17 — Th (ppm) estimation based on EWBA and ICSM methods (S8 to S10) Log scale for normalizing the concentrations (actual values mentioned inside bars in ppm)

full-spectrum fitting in resolving overlapping photo peaks and mitigating background driven variance that is not adequately handled by fixed energy window methods.

While the absolute concentration values obtained using EWBA and ICSM for the samples are generally comparable and remain within expected statistical agreement, ICSM consistently produces tighter confidence intervals. This improvement is particularly evident in samples characterized by moderate spectral complexity or elevated background levels. For example, in sample S2, the uncertainty in uranium

Table 2 — Deviation between K, U and Th values obtained ICSM and EWBA

Sample No.	K (%)		U (ppm)		Th (ppm)	
	Absolute Deviation (%)	Percentage Deviation (%)	Absolute Deviation (ppm)	Percentage Deviation (%)	Absolute Deviation (ppm)	Percentage Deviation (%)
S1	0.00	0.0	6	6.0	15	3.9
S2	0.20	12.8	21	3.5	3	11.5
S3	0.10	2.9	10	4.8	3	21.4
S4	0.30	11.6	6	1.9	2	22.2
S5	0.35	18.0	12	3.1	2	28.6
S6	0.22	35.5	3	9.1	12	3.6
S7	0.64	12.7	8	12.7	3	4.0
S8	4.06	91.0	48	1.3	71	82.5
S9	0.08	7.4	9	6.2	124	2.6
S10	0.07	31.8	10	1.0	2	50.0

Table 3 — Table showing precision enhancement in ICSM approach

Sample No.	Error in K (%)			Error in U (ppm)			Error in Th (ppm)		
	EWBA	ICSM	Error Reduction (%)	EWBA	ICSM	Error Reduction (%)	EWBA	ICSM	Error Reduction (%)
S1	0.18	0.08	55.6	2.43	1.39	42.8	7.47	3.31	55.7
S2	0.62	0.34	45.2	6.00	2.50	58.3	5.80	2.89	50.2
S3	0.30	0.20	33.3	2.88	1.37	52.4	3.11	2.00	35.7
S4	0.39	0.24	38.5	3.79	1.68	55.7	3.43	2.14	37.6
S5	0.45	0.27	40.0	4.32	1.88	56.5	3.85	2.31	40.0
S6	0.21	0.14	33.3	1.80	1.03	42.8	6.79	2.72	59.9
S7	0.20	0.15	25.0	1.60	0.84	47.5	3.54	1.91	46.1
S8	2.89	1.48	48.8	27.62	10.42	62.3	25.97	6.07	76.6
S9	1.49	0.56	62.4	11.32	4.99	55.9	51.14	19.92	61.1
S10	0.92	0.51	44.6	8.97	3.76	58.1	0.21	0.15	28.6

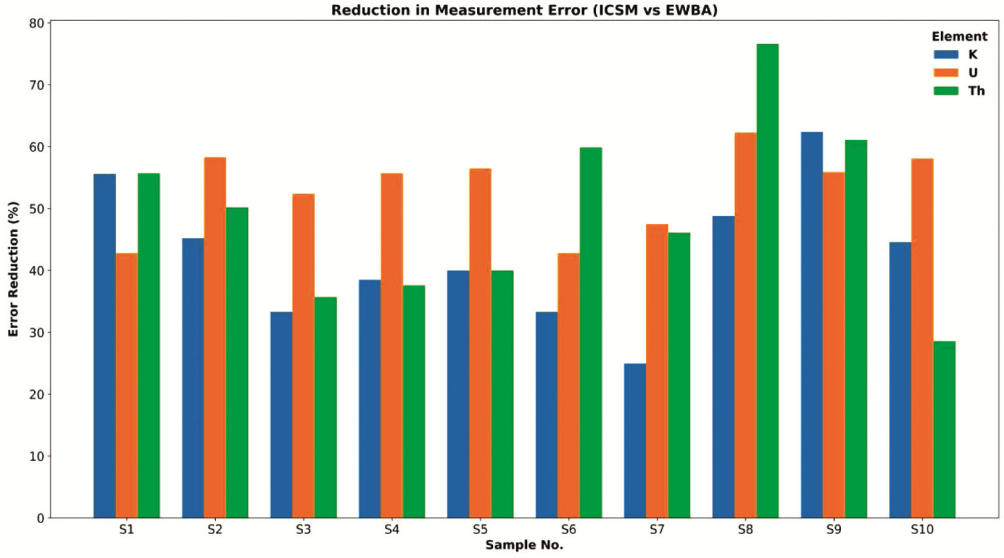

Fig. 18 — Error reduction (%) in potassium (K), uranium (U), and thorium (Th) across samples

decreases from ±6.0 ppm (EWBA) to ±2.5 ppm (ICSM), while the thorium uncertainty decreases from ±5.8 ppm to ±2.89 ppm. Similar trends are observed across all samples, indicating a systematic enhancement in measurement precision rather than isolated improvements.

The in-house reference standards (S8 – S10) provide an independent evaluation of both precision and quantitative reliability. When treated as unknown samples, ICSM not only yields significantly lower uncertainties than EWBA but also produces concentration estimates that are in closer agreement with independently determined high-purity germanium (HPGe) detector reference values (particularly for the dominant radionuclide in each standard). For instance, in sample S8 (which is uranium rich) the uranium uncertainty is reduced from ±27.62 ppm (EWBA) to ±10.42 ppm (ICSM). Similarly, in sample S9, dominated by thorium, the thorium uncertainty decreases from ±51.14 ppm to ±19.92 ppm, and in sample S10, the uranium uncertainty is reduced from ±8.97 ppm to ±3.76 ppm.

These results demonstrate that the uncertainty reduction achieved by ICSM is not merely statistical but is accompanied by improved quantitative agreement with high-resolution reference measurements. The combined evidence from geological samples and in-house standards confirms that ICSM provides a more precise and statistically robust technique for quantitative gamma ray spectrometric analysis. To further assess quantitative reliability, a direct comparison of HPGe reference concentrations with those obtained using EWBA and ICSM is presented in Table 4.

For uranium, both EWBA and ICSM reproduce the HPGe reference concentrations with good accuracy across all three standards. However, ICSM consistently achieves this agreement with markedly reduced uncertainty, as demonstrated earlier. For thorium, particularly in the high Th standard S9, ICSM provides concentrations closer to the HPGe reference than EWBA, which exhibits a tendency toward overestimation. In the case of potassium, both methods show larger deviations from HPGe values, reflecting the inherent limitations of NaI(Tl) detectors at lower energies. Nevertheless, ICSM avoids the severe overestimation observed with EWBA in mixed radionuclide samples such as S8. These results demonstrate that the uncertainty reduction achieved by ICSM is accompanied by comparable or improved agreement with independently measured HPGe concentrations. The improvement is therefore not only statistical but physically meaningful, confirming the robustness of the full-spectrum, iteratively weighted chi-square approach for quantitative gamma ray spectrometric analysis.

Since each physical sample is measured using two methods (EWBA and ICSM) and an associated measurement uncertainty (error) is reported for each method. Therefore, the paired t-test is performed to evaluate whether the mean difference between two sets of paired observations is statistically different from zero. As the two error values for each sample correspond to the same sample, these observations are paired (dependent). The paired t-test thus directly tests whether the ICSM method yields on average smaller errors than EWBA across the same set of samples. A statistically significant result ($p < 0.05$) indicates that the observed mean difference is unlikely to be due to random sampling alone and supports the conclusion that one method consistently produces different (in this case lower) uncertainty.

For each sample k ($k = 1 \ldots n$) we have two uncertainty estimates $\text{Error}_{\text{EWBA},k}$ and $\text{Error}_{\text{ICSM},k}$, where, only the uncertainty (the "±" value) is used in the test. For each sample the difference is computed as mentioned below:

$$d_k = \text{Error}_{\text{EWBA},k} - \text{Error}_{\text{ICSM},k} \quad \ldots (20)$$

Positive values of d_k indicate that EWBA error > ICSM error for that sample.

Next, the sample mean of the differences $\bar{d}$ and the sample standard deviation S_d are computed. The paired t statistic is:

Table 4 — Comparison of HPGe reference concentrations with EWBA and ICSM results for in-house standards

Sample	Method	K (%)	U (ppm)	Th (ppm)
S8	HPGe	1.20	3630	11
	EWBA	4.46	3576	86
	ICSM	0.40	3624	15
S9	HPGe	1.80	148	4694
	EWBA	1.08	145	4743
	ICSM	1.00	136	4619
S10	HPGe	0.40	1016	5
	EWBA	0.22	1026	4
	ICSM	0.15	1036	2

Table 5 (a) — Paired t-test Results (Full Dataset: S1–S10, including CRMs)

Element	t-statistic	p-value (two-tailed)	Degrees of Freedom	Interpretation
K (%)	2.58	0.029	9	Statistically significant
U (ppm)	2.60	0.029	9	Statistically significant
Th (ppm)	2.08	0.067	9	Marginal significance

Table 5 (b) — Paired t-test Results (Reduced Dataset: S1–S7, excluding CRMs S8–S10)

Element	t-statistic	p-value (two-tailed)	Degrees of Freedom	Interpretation
K (%)	4.47	0.004	6	Highly significant
U (ppm)	4.57	0.004	6	Highly significant
Th (ppm)	4.80	0.003	6	Highly significant

Table 6 — Shapiro–Wilk Normality Test for Paired Differences

Element	W-statistic	p-value	Conclusion
K (%)	0.81 (approx.)	< 0.01	Non-normal
U (ppm)	0.78 (approx.)	< 0.01	Non-normal
Th (ppm)	0.75 (approx.)	< 0.01	Non-normal

$$t = \frac{\bar{d}}{s_d/\sqrt{n}} \quad \ldots (21)$$

Under the null hypothesis (mean difference = 0), t follows a t distribution with n – 1 degrees of freedom. A two-tailed p-value is obtained from the t distribution. If $p < \alpha$ (commonly 0.05), we reject the null hypothesis and conclude a statistically significant mean difference between methods. The p-value and the interpretation presented in the Tables 5 (a) and (b) highlights the superiority of ICSM over EWBA in precision estimate.

3.4 Interpretation and Validity of the Test

The paired t-test analysis demonstrates that the ICSM method consistently reduces estimation uncertainty relative to EWBA across all samples. For the full dataset, statistically significant improvements are observed for potassium and uranium, while thorium shows marginal significance due to increased variability in high-activity CRM samples. When these CRMs are excluded, all three elements exhibit statistically significant improvements, confirming the intrinsic effectiveness of the ICSM approach under typical measurement conditions. Importantly, the inclusion of CRMs provides a more stringent and realistic evaluation of the method, as these samples represent challenging scenarios with strong spectral overlap and higher statistical fluctuations. The observed behavior is therefore not a limitation of the ICSM method, but rather a reflection of the underlying physical constraints of gamma-ray spectrometry.

Overall, the combined analysis confirms that ICSM provides a robust and statistically reliable improvement in uncertainty estimation, while maintaining stability across both standard and extreme measurement conditions. The assumptions underlying the paired t-test were evaluated using numerical method. Normality of the paired differences was assessed using the Shapiro–Wilk test, which indicated deviations from normality for all three elements (Table 6). This deviation arises primarily from high-activity samples (S8–S10), which introduce skewness in the distribution. However, the paired t-test is known to be robust to moderate deviations from normality, particularly when the differences exhibit a consistent direction, as observed in the present study.

4 Conclusion

Iterative chi-square minimization with adaptive uncertainty refinement provides a robust and statistically efficient approach for quantifying K, U and Th concentrations in geological samples using gamma ray spectrometry. Under identical counting conditions, the ICSM method consistently achieves substantially lower uncertainties than conventional Energy Window Based Analysis (EWBA), demonstrating the advantage of full spectrum modeling over fixed energy window techniques.

The improvement in precision is statistically significant for all three elements, as confirmed by paired t-tests, indicating that the observed uncertainty reductions are systematic rather than due to random variability. Validation using in-house reference standards with independently determined HPGe concentrations further shows that ICSM yields

concentration estimates in comparable or improved agreement with reference values while maintaining markedly reduced uncertainties, particularly for uranium and thorium.

Overall, the superior performance of ICSM arises from its weighted least squares formulation, full spectrum fitting and iterative uncertainty updating based on expected counts. These characteristics make ICSM a rigorous and reliable alternative to EWBA for applications requiring high precision and statistically defensible elemental quantification.

Recent advances in spectral deconvolution offer several opportunities to extend the full-spectrum analysis framework presented in this study. Incorporation of Bayesian inference would provide a unified probabilistic treatment of Poisson counting statistics, background uncertainty, and parameter correlations. Such an approach could be implemented using Markov Chain Monte Carlo or variational inference to jointly estimate concentrations, calibration parameters and background components.

Additional improvements may be achieved through machine learning based spectral processing. Neural networks trained on Monte Carlo simulated spectra have shown promise for spectral denoising, mitigation of peak overlap, and rapid spectrum to nuclide mapping. These methods could be used either as a preprocessing step or to provide initial concentration estimates that are subsequently refined using physically constrained chi-square or Bayesian models.

Finally, the methodology is readily transferable to other detector systems. By constructing detector specific response matrices and incorporating effects such as escape peaks, intrinsic background and detailed energy resolution functions, the framework can be extended to high-resolution detectors such as HPGe and $LaBr_3$:Ce, enabling a flexible platform for both laboratory based and field deployed gamma ray spectrometry.

The iterative chi-square minimization approach relies on detector response functions derived from calibration standards, which represent an idealized approximation of detector behavior. Variations in energy resolution, peak shape, scattering geometry and temporal effects such as thermal instability and electronic gain drift may not be fully captured, leading to mismatches between measured and modeled spectra. Background subtraction applied prior to fitting for consistency with response functions, alters Poisson counting statistics and introduces additional variance and inter channel correlations that are not explicitly modeled.

The weighted least squares formulation further assumes statistical independence of spectral channels, whereas finite detector resolution inherently couples adjacent channels, particularly in regions of spectral overlap or low count rates. Although the adaptive uncertainty model partially compensates for these effects through variance inflation, it does not provide a full treatment of channel covariance. The present implementation is limited to K, U and Th and does not explicitly model additional radionuclides or detector-specific features such as escape peaks, which may require expanded response modeling in future applications.

References

1 Killeen P G, Gamma ray spectrometric methods in uranium exploration application and interpretation, in: Geophysics and geochemistry in the search for metallic ores, edited by P J Hood (Geological Survey of Canada, Economic Geology Report 31), 1979, pp. 163–229.

2 Knoll G F, Radiation detection and measurement, 4th Edn (Wiley, New York), 2010.

3 Gilmore G, Practical gamma ray spectrometry, 2nd Edn (Wiley, Chichester), 2008.

4 Trombka J I, Least-square analysis of gamma ray pulse height spectra, Jet Propulsion Laboratory Technical Report No. 32-373, Pasadena, CA, 1962.

5 Guidelines for radioelement mapping using gamma ray spectrometry data, IAEA-TECDOC-1363 (International Atomic Energy Agency, Vienna), 2003.

6 Burrus C S, Iterative reweighted least squares (OpenStax CNX), 2012.

7 Mann B J, Least squares analysis of gamma ray spectra, Technical Publication TP-414, 1967.

8 Cash W, *Astrophys J*, 228 (1979) 939.

9 Andrae R, Schulze-Hartung T & Melchior P, Dos and don'ts of reduced chi-squared, arXiv:1012.3754, 2010.